Contemporary Physics, 1997, volume 38, number 4, pages 269–288

Simulating the geodynamo

GARY A. GLATZMAIER* and PAUL H. ROBERTS†

Three-dimensional numerical simulations of convection and magnetic field generation in the Earth's core now span several hundred thousand years; the magnetic field created during most of this time has an intensity, structure and time dependence similar to the present geomagnetic field. Five models are described here. The first is a homogeneous Boussinesq model, driven steadily by heat sources on the inner core boundary. At about 36 000 years into the simulation, a reversal of the dipole moment occurs that resembles those seen in the paleomagnetic reversal record. The four subsequent models are inhomogeneous, that is they allow for the varying properties of the Earth with depth. They are also evolutionary, in that they are powered by the secular cooling of the Earth over geological time. This cooling causes the inner core to grow through freezing, with the concomitant release at the inner core boundary of not only latent heat of crystallization but also light constituents of core fluid that provide respectively thermal and compositional sources of buoyancy that maintain core convection. The behaviour of these models depends on what is assumed about the heat flux from the core into the mantle. Two of the models studied are superadiabatic, that is they postulate that the heat flux from the core exceeds the flux that thermal conduction alone would allow; two are subadiabatic, where the opposite is assumed. In two of the models it is supposed that the heat is extracted uniformly across the core–mantle boundary; in the other two, substantial horizontal variations are allowed, the precise choice of which is guided by the seismically inferred lower mantle tomography. The very different behaviours of the four models are described here. Reasons are given why, for the homogeneous model and for the two superadiabatic models, the solid core should rotate faster than the mantle by a couple of degrees per year, our prediction for the Earth that was subsequently supported by two independent seismic analyses.

1. Introduction

It has been known for centuries that the Earth is magnetic, and throughout that time man has puzzled over why that should be. The directional property of the magnetic field, which has been such a boon to mariners, also spawned the first 'theory': the magnetic compass needle points towards the pole star. This idea did not survive the publication in 1600 of the world's first scientific treatise, 'De Magnete'. Its author, William Gilbert, was, for the last two years of his life, the principal court physician to Queen Elizabeth the First of England. His work contained the results of his terrella or 'little Earth' experiment, which showed that the direction of the magnetic field on the surface of a sphere of lodestone, his terrella, was similar to the direction of the geomagnetic field at corresponding latitudes on the Earth's surface, insofar as it was known in his day. Chapter 1 of the sixth book of his treatise is entitled (in Latin) 'On the Globe of the Earth, the Great Magnet'.

In 1838 Gauss provided mathematical teeth to Gilbert's claim that the origin of the Earth's field lay within it. In the poorly conducting environs of the Earth's surface, the magnetic field $\mathbf{B}$ is the gradient of a scalar potential satisfying Laplace's equation:

$$\mathbf{B} = -\nabla V, \qquad \nabla^2 V = 0.$$

The potential is the sum of V_I, produced by sources within the Earth, and V_E created outside the Earth. The former is a sum of multipolar terms of the form

$$-\mathbf{m}\cdot\nabla r^{-1},\ -(\mathbf{m}_1\cdot\nabla)(\mathbf{m}_2\cdot\nabla)r^{-1},$$
$$-(\mathbf{m}_3\cdot\nabla)(\mathbf{m}_4\cdot\nabla)(\mathbf{m}_5\cdot\nabla)r^{-1}\ldots, \qquad (1)$$

Communicating Author's address: Institute of Geophysics and Planetary Physics, MS C305 Los Alamos National Laboratory, Los Alamos, NM 87545, USA.
†*Author's address:* Institute of Geophysics and Planetary Physics, Center for Earth and Planetary Interiors, Geology Building, UCLA, 405 Hilgard Avenue, Los Angeles, CA 90095-1567, USA.

that increase with depth; the latter is a sum of terms

$$-\mathbf{r}^3\mathbf{e}\cdot\nabla r^{-1},\ -r^5(\mathbf{e}_1\cdot\nabla)(\mathbf{e}_2\cdot\nabla)r^{-1},$$
$$-r^7(\mathbf{e}_3\cdot\nabla)(\mathbf{e}_4\cdot\nabla)(\mathbf{e}_5\cdot\nabla)r^{-1}\ldots, \qquad (2)$$

that decrease with depth, i.e. both increase in the direction of their respective sources; here r is the distance from the centre of the Earth, O. The vectors $\mathbf{m}$, $\mathbf{m}_1$, $\mathbf{m}_2$, ... and $\mathbf{e}$, $\mathbf{e}_1$, $\mathbf{e}_2$, ... are constant. Fitting the sums (1) and (2) to the data available to him, Gauss found that V_E is negligible compared with V_I. From now on we consider V_I alone, writing it simply as V. Moreover, we shall restrict ourselves to the first 12–13 terms of (1), the remaining terms being contaminated by crustal sources of no concern to us here. (See, for example, section 5 of Langel (1986).)

The first term in (1), known as the *centred dipole*, dominates the remainder; it accounts for typically over 80% of the observed field. The component, m_z, of $\mathbf{m}$ parallel to the Earth's rotation axis, Oz, provides the *axial dipole*, which at present is about 5 times larger than the equatorial dipole, $\mathbf{m}$-$m_z\hat{\mathbf{z}}$, where $\hat{\mathbf{z}}$ is the unit vector parallel to Oz. The *geomagnetic axis* is the line through O parallel to $\mathbf{m}$; today it is within about 10° of the geographical axis. The geomagnetic axis meets the Earth's surface at the *geomagnetic poles*. Their proximity to the geographic poles is what gives the compass needle its directional property. The *geomagnetic dipole moment* is the magnitude m of $\mathbf{m}$. Currently it is about 8×10^{22} A m^2. When the first term is subtracted from the sum of the multipoles (1), the remnant defines the *non-dipole field*. This is dominated by the quadrupolar contributions that involve $\mathbf{m}_1$ and $\mathbf{m}_2$. The variations in the non-dipole field over the Earth's surface are therefore of continental scale. If the non-dipole field were absent, one would be able to infer from the strength and direction of $\mathbf{B}$ at any point P on the Earth's surface what $\boldsymbol{m}$ is in magnitude and direction. If one ignores the non-dipole field and carries out the calculation anyway, one obtains a *virtual dipole moment* (VDM) and *virtual geomagnetic poles* (VGPs). These vary with the location of P but, because of the dominance of the centred dipole, they do not depart far from the geomagnetic dipole moment and poles; to avoid confusion, the latter are sometimes called the *true geomagnetic moment* (TGM) and the *true geomagnetic poles* (TGPs) to distinguish them from the VDMs and VGPs deduced at different points on the Earth's surface; these will be considered further in section 7.

Gilbert's idea that the Earth is a magnet became untenable within two decades of his death in 1603. Edmund Gunter noticed that the difference in the directions of the field in 1580 and at a neighbouring site in 1624 seemed too great to be explained by observational error. But Gilbert had written that the Earth's field is unchanging, and so great was his authority that Gunter made no claim. The discovery of what is now called 'the secular variation' was first announced in 1635, by Henry Gellibrand. The adjective 'secular' has come to mean not only that the variations are slow, having time scales that range from decades to millenia, but also that their origin lies within the Earth. Short period variations exist but are mostly created by the Sun and, as they are externally produced, they are of no concern to us here. Before the turn of the 17th Century, a persistent feature of the secular variation had been recognized: a slow westward drift of the field patterns. Edmund Halley, of comet fame, presciently surmised that this meant that the interior of the Earth is in motion relative to the crust. The westward drift is far from uniform over the globe; at some places and at some times, it may even be eastward. For a detailed discussion of the secular variation and westward drift, see Langel (1986).

The 20th Century has seen the birth and explosive growth of paleomagnetism, the study of the magnetism trapped in rocks at the time of their formation. As a result, it is now known that the Earth has possessed a magnetic field for at least the last 3·3 billion years, that the strength of the field, as assessed from VDMs, has averaged 9×10^{22} A m^2, and that is has rarely deviated from the average by as much as an order of magnitude. The dipole moment experiences secular variation and, at the time Gauss carried out his analysis, m was about 50% greater (12×10^{22} A m^2) than at present. The average VGP positions during the past few million years coincide with the geographical poles.

The early and astounding success of paleomagnetism was the discovery that the remnant magnetization of rocks and the field directions at the sites at which they were collected are sometimes oppositely oriented. The obvious inference is that, at times in the past, the polarity of the geomagnetic field has been reversed. If we could transport a magnetic compass needle to such an epoch, its North seeking end would point South and not North! This revolutionary interpretation was not immediately accepted, partly because, as Uyeda discovered in 1958, self-reversing rocks exist. It is by now convincingly established, however, that polarity reversals have happened often and irregularly throughout geological time, and that each takes 3–5 thousand years to complete. During the present geological epoch, they have occurred every 200 000 years on average, although the last reversal took place about 720 000 years ago. Much longer periods of one polarity dominated the Cretaceous and the Permian. The polarity record shows no discernible preference for one polarity over the other.

It is worth pausing here to summarize some of the more important questions that a viable theory of geomagnetism should aspire to answer:

Q1 Why is the Earth magnetic?
Q2 Why has its magnetic field existed over at least 70% of geological time?
Q3 Why is it predominantly dipolar?

Q4 What determines its strength?
Q5 Why does its strength vary, but by so little?
Q6 Why does the magnetic compass needle point approximately North?
Q7 Why does the averaged geomagnetic axis coincide with the geographical axis?
Q8 Why does the polarity of the Earth's field reverse?
Q9 What happens to the geomagnetic field during a reversal and why?
Q10 Why does the frequency of reversals vary so greatly over geological time?
Q11 Why is neither polarity of field favoured over the other?
Q12 What causes the slow secular change of the field?
Q13 What is the significance of the westward drift?
Q14 Can a single mechanism explain why other planets and satellites are magnetic too?

In what follows, we shall frequently refer back to these questions and try to assess how far they have been successfully answered. A plausible answer to Q3 was given long ago. In so far as sources of field are absent, the expression of **B** as a sum of multipoles (1) holds even below the Earth's surface, and clearly demonstrates that the dominance of the dipole over the remaining multipoles diminishes with radius r. All terms become comparable in size at a depth of order 3000 km. This *suggests* that significant sources of **B** do not exist in the Earth's mantle, and that the origin of the geomagnetic field lies in the Earth's core, the surface of which, called 'the core–mantle boundary' (CMB), lies at about this depth ($r = r_{CMB} \approx 3480$ km). Stated differently, the fact that the horizontal scale of the non-dipole field at the Earth's surface is of continental dimensions, suggests that the sources of **B** are at a similar or greater depth within the Earth.

This answer to Q3 is reinforced by partial answers to Q12 and Q13. The time scale of the secular variation is long compared with those of most atmospheric and oceanic phenomena but short compared with those of most geological processes. It might nevertheless be characteristic of motions of the fluid core. This thought also potentially vindicates Halley's explanation of the westward drift in terms of fluid motions, although of course the existence of a fluid core was not known until 1906, and the reason why the westward drift should be opposite to that of weather patterns in the Earth's atmosphere is far from apparent.

The central question is Q1. Polarity reversals and the secular variation not only rule out Gilbert's permanent magnetism theory; they also make it hard to believe Blackett's alternative proposal, that every body has, through its rotation, an intrinsic magnetic field whose dipole moment is proportional to the angular momentum of the body. There remains only one possibility: the geomagnetic field is created by electric currents flowing within the Earth, for it has been known since the time of Oersted that where there is electric current there is also magnetic field; a very simple case is sketched in figure 1. Moreover the core is thought to be composed largely of iron, which is a good electrical conductor; its conductivity, σ, is usually estimated to be about 4×10^5 S m^{-1}. But there is a difficulty: unless the electric currents are maintained in some way, they and their attendant magnetic fields will disappear in an 'ohmic diffusion time', $\tau_\sigma = \mu\sigma r_{CMB}^2$. This time scale emerges from the dimensional analysis of (3) below, with **V** set zero. Because of the high temperature of the Earth's interior, the magnetic permeability μ is thought to be that of free space ($\mu_0 = 4\pi \times 10^{-7}$ H m^{-1}). For the Earth's core, τ_σ is at most a few tens of thousands of years, which is very small compared with the age of the geomagnetic field. To explain the Earth's magnetism by electric currents, one must provide a source for those currents.

Naturally one thinks first of some kind of electrochemical effect, i.e. a battery, but on closer scrutiny it appears that such sources are not potent enough, and the same seems to be true of thermoelectric effects. And in both cases it would be hard to answer Q8. Following the original suggestion of Joseph Larmor (1919), it is now generally believed that the electric currents are maintained by fluid motions in the Earth's electrically conducting core, in much the same way as in a self-excited electricity generator, or 'dynamo'. Today self-excited dynamos are commonly invoked to explain the magnetism of cosmic bodies such as the Sun and solar-type stars, those planets and Jovian satellites known to possess magnetic fields, and those galaxies that are magnetic. In other words, the answer to Q14 is, 'Yes'. The study of the field generation process is called 'dynamo theory'. One telling advantage that geodynamo theory enjoys over all hypotheses is its success in answering Q11; see section 4 below.

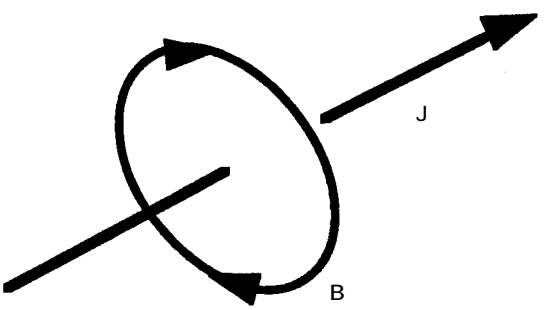

Figure 1 The magnetic field B created by a line current J. The field is in a right-handed sense about the direction of current flow.

Unlike the commercial dynamo, where interest centres on the electric currents that can be led from the generator to sites where they can do useful work such as lighting a room or turning an electric motor, and where the associated magnetic fields are of subsidiary importance, geodynamo theory centres on the fields and not on the currents. Although it appears that the currents produced by the geodynamo operate an electric motor in the core (see section 5), they uselessly squander an enormous amount of electrical energy, perhaps as much as 200 000 MegaWatts, i.e. 0·2 TeraWatts (0·2 TW). From where does the dynamo acquire this energy?

2. The inner core: as big as the Moon; as hot as the Sun

Based on the wealth of seismic data available, very detailed models of the Earth's internal structure have been developed, one of the best known of which is the Preliminary Reference Earth Model of Dziewonski and Anderson (1981), generally known as 'PREM'. In this and other models, the core is an adiabatic, hydrostatic, spherically-symmetric body, the slight flattening of the equi-density surfaces created by centrifugal forces being ignored. The other forces acting on the fluid outer core ('FOC') are even smaller, and do not significantly disturb the hydrostatic balance. Convective motions in the FOC are sufficiently vigorous to mix the fluid thoroughly, so maintaining the adiabatic (or isentropic) state. The increase of horizontally averaged pressure, $\overline{p}$, with depth is accompanied by increases in the horizontal averages, $\overline{T}$ and $\overline{\rho}$, of the temperature and density. It is estimated that $\overline{T}$ at the inner core boundary ('ICB'), which is the surface of the solid inner core ('SIC'), is within $\pm 20\%$ of 5300 K, or much the same temperature as the surface of the Sun. The radius, r_{ICB}, of the SIC is 1222 km, which is 35% of the outer radius of the FOC, or about 70% of the radius of the Moon.

The decrease of $\overline{T}$ with distance r from the geocentre implies a conductive heat flux into the mantle of about 5 TW but, because of convection in the FOC, the actual rate at which heat leaves the core may be greater or less than this; it is not yet known which. Perhaps indeed the question will first be decided by studies of the geodynamo such as those described here. Both superadiabatic and subadiabatic states will be considered in section 8 below.

More than 40 years ago, Jack Jacobs (1953) argued that the inner core is the result of freezing of core fluid during the general cooling of the Earth since its creation. This hypothesis has stood the test of time. It may at first sight seem strange that when the core is cooled at the top it would freeze at the bottom, but the increasing pressure with depth in the core raises the freezing temperature more rapidly than the adiabatic temperature. According to PREM, $\overline{\rho}$ rises from $9{\cdot}9 \times 10^3$ kg m^{-3} at the CMB to $13{\cdot}1 \times 10^3$ kg m^{-3} at the geocentre, O. At the ICB there is a density jump of $\Delta\overline{\rho} \approx 0{\cdot}6 \times 10_3$ kg m^{-3}, from $12{\cdot}2 \times 10^3$ kg m^{-3} in the fluid to $12{\cdot}8 \times 10^3$ kg m^{-3} in the solid. Partially because these densities are approximately that of pure iron at the appropriate pressures, the core is usually thought to be predominantly made of iron. Nevertheless, the density of the FOC is less than that expected for pure iron, and is also less than that of the SIC. This is interpreted to mean that the fluid iron is alloyed with lighter elements. There is as yet no consensus as to which light element predominates, the competing merits of sulphur, silicon and oxygen being vigorously but inconclusively argued by their various proponents. The simplest view, taken by Stanislav Braginsky (1964) and by ourselves, is that the core is essentially a binary alloy, and we denote the mass fraction of the light constituent (whatever it is) by ξ. Generally an alloy will not preserve its chemical composition when it freezes, and on the available evidence the SIC is richer in iron that the FOC. Then the density jump $\Delta\overline{\rho}$ is due not only to contraction of the fluid on freezing ($\Delta\overline{\rho}_\ell$), but also to an increase, $\Delta\overline{\rho}_\xi$, arising from the decrease, $\Delta\xi$, in $\overline{\xi}$ during freezing.

As the Earth cools, further material freezes onto the ICB and the SIC grows, but only at a rate of order 10^{-12}–10^{-11} m s^{-1}. As fluid freezes onto the ICB, not only is the heat of crystallization released, which heats the adjacent fluid and makes it buoyant, but also the light constituent of the alloy, which is buoyant too. The compositional source of buoyancy, first suggested by Braginsky (1963), may be stronger than the thermal source and will augment it. Compositional buoyancy acquires its energy gravitationally from the ever increasing central condensation of mass as the inner core freezes. Together, the two energy sources amply suffice to make good the ohmic energy expense of the dynamo. This answers Q2.

3. Self-excited dynamo action

Dynamo theory at first advanced slowly after Larmor's original suggestion. The first results were not encouraging. In 1933, Thomas Cowling proved a celebrated theorem: axisymmetric magnetic fields cannot be maintained by dynamo action. It was not until 1958 that Arvid Herzenberg and George Backus independently showed that self-sustaining fluid dynamos can exist, although the models they produced were too artificial to be geophysically realistic. Nevertheless an important point of principle had been settled. The reader may well ask, 'Why was it so important? The existence of generators of electricity in power stations suffices to prove that self-excited dynamos exist'. This, however, begs the question. The man-made dynamo is an intricate construction in which the current paths and motions are deliberately designed to ensure efficient conversion of mechanical energy to electrical

energy. The machine is strongly asymmetric. More precisely it is not mirror-symmetric, i.e. the mirror image of the machine differs from the machine itself, in the same way that the thread on an ordinary wood screw appears reversed when viewed in a mirror. In contrast, the Earth's fluid core is an approximately spherical mass of fluid that is maintained in an almost homogeneous state by convective motions; structurally it is a mirror-symmetric system. One might be forgiven for thinking that even if electric currents were produced they would be short-circuited so effectively that any nascent dynamo action would be stillborn. In short, the question that should be asked is not whether self-excited dynamos exist (they obviously do), but whether self-excited dynamos can operate in, for instance, a spherical mass of nearly *homogeneous* fluid. This was the question that Herzenberg and Backus answered in the affirmative. But there remained the daunting task of finding geophysically realistic models.

All early theorists seeking realism focused, as had Herzenberg (1958) and Backus (1958), on kinematic dynamos. Here the word 'kinematic' is used in the sense of classical mechanics to mean that there is no attempt to satisfy the dynamics of fluid flow; only the electrodynamics is attacked. The fluid velocity, **V**, is specified in some plausible way and Maxwell's equations (or more precisely the pre-Maxwell equations, since displacement currents are negligibly small) are solved. After mathematically substituting expressions for the electric field **E**, and the electric current density **J**, the so-called 'induction equation' is obtained, governing the magnetic field, **B**:

$$\frac{\partial \mathbf{B}}{\partial t} = \nabla \times (\mathbf{V} \times \mathbf{B}) - \nabla \times (\bar{\eta} \nabla \times \mathbf{B}) \qquad (3)$$

the solution to which must exclude all sources of field external to the core. Clearly, if (as must be the case)

$$\nabla . \mathbf{B} = 0 \qquad (4)$$

initially then, according to (3), it is true for all times t. The final term in (3) represents the ohmic loss of magnetic energy to heat; $\eta = 1/\mu_0 \sigma$ is the magnetic diffusivity. The penultimate term in (3) represents the conversion of mechanical energy to magnetic energy through electromagnetic induction, the process that creates an electromotive force (or emf), $\mathbf{V} \times \mathbf{B}$, when a conductor moves with velocity **V** in a magnetic field **B**. This emf features in Ohm's law, which is no longer $\mathbf{J} = \sigma \mathbf{E}$, but is $\mathbf{J} = \sigma (\mathbf{E} + \mathbf{V} \times \mathbf{B})$. In a working dynamo, electromagnetic induction must be able to transform kinetic energy into magnetic energy fast enough to offset the ohmic losses. This requires that **V** should be 'big enough', or more precisely that the magnetic Reynolds number

$$\mathrm{Rm} = \frac{V r_{\mathrm{CMB}}}{\bar{\eta}}$$

must be of order 1 or greater, where V is a characteristic flow speed. What Cowling's (1933) theorem, and a number of later 'anti-dynamo theorems', established was that the condition $\mathrm{Rm} > O(1)$ is necessary for dynamo action but is far from sufficient. The focus of kinematic theory became, 'What else is required of the fluid velocity to make the dynamo work?'

The most important finding of kinematic theory may have been the demonstration that fluid motions in efficient dynamos lack mirror-symmetry. It is as though the motions have to supply, by their own lack of symmetry, the absence of mirror-symmetry so essential in the commercial generator and so obviously missing from a homogeneous mass of fluid. And, what is exciting is that, through the action of the Coriolis acceleration $-2\Omega \times \mathbf{V}$, where Ω is the angular velocity, the motions in a convecting mass of fluid such as the Earth's core necessarily lack mirror-symmetry. An example of this is the so-called 'thermal wind'. In the simplest case, sketched in the upper part of figure 2, we imagine that an upwelling convective plume, axisymmetric with respect to the rotation axis NS, carries heat from the northern hemisphere of the ICB to the northern hemisphere

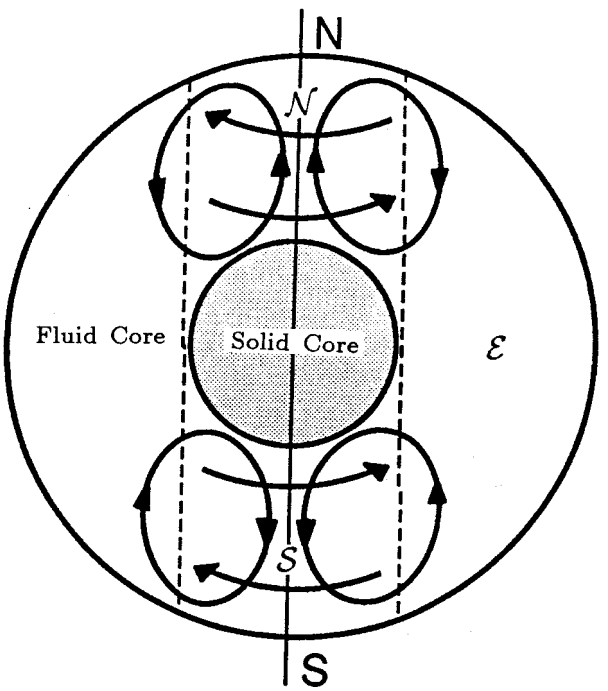

Figure 2. A sketch of axisymmetric meridional circulations from ICB to CMB in the tangent cylinder, in the northern and southern hemispheres of the fluid core. Because of rotation, these produce zonal thermal winds in the directions indicated. The dashed line shows the (imaginary) tangent cylinder which separates the fluid core into an external part $\mathcal{E}$ and two internal parts, $\mathcal{N}$ and $\mathcal{S}$, lying North and South of the solid inner core; see also section 5.

of the CMB; the fluid returns from CMB to ICB along streamlines further away from NS. In doing so it moves away from NS when near the CMB, but towards NS when near the ICB, and in these parts of the circulation, in which the component of $\mathbf{V}$ perpendicular to Ω is significant, the Coriolis force creates an axisymmetric zonal motion that is prograde (eastward) near the ICB and retrograde (westward) near the CMB, relative to the solid mantle above. These flows encircling the NS axis are known as 'thermal winds'. Like the trade winds in the Earth's atmosphere, they owe their existence entirely to the 'deflection' of the meridional circulations by the Coriolis force. Similar thermal winds are created when Coriolis forces act on a rising plume in the southern hemisphere of the FOC, as sketched in the lower part of figure 2.

The example just given illustrates another important feature of flows in rotating fluids: the creation of *helicity* by the Coriolis force. Helicity is defined as

$$H = \mathbf{V} \cdot \omega,$$

where $\omega = \nabla \times \mathbf{V}$ is the vorticity of the flow. The zonal circulations encountered above are associated with an ω that is in the S$\rightarrow$N direction near the ICB and in the N$\rightarrow$S direction near the CMB. Since $\mathbf{V}$ is outwards (at least near NS), H is positive in the northern hemisphere near the ICB but negative near the CMB; the reverse is true for the corresponding flows in the southern hemisphere. Helical flows are effective in maintaining magnetic field.

In 1942, Hannes Alfvén became interested in how the Sun creates and maintains its magnetic field. He discovered a completely new field of research: magnetohydrodynamics, or MHD for short. He proved an interesting theorem concerning magnetic lines of force. These are imaginary curves that are everywhere parallel to $\mathbf{B}$; they have been useful aids to thought ever since they were introduced by Michael Faraday in the nineteenth century. Alfvén (1942) showed that a perfect electrically conducting fluid ($\sigma = \infty$, or equivalently $\eta = 0$ or $\mathrm{Rm} = \infty$) carries magnetic lines of force with it in its motion, just as though those lines were 'frozen' to it. The Earth's core is not a perfect conductor but, at least when considering fields of r_{CMB} scale, Rm is large and Alfvén's theorem is useful in predicting qualitatively the effect of a motion on a magnetic field. For example, returning to figure 2, we may imagine that there is an axisymmetric magnetic field threading the core from South to North. Thanks to Alfvén's theorem, we may confidently assert that the thermal wind will drag the field lines round the rotation axis in a process reminiscent of winding a watch spring. This induced magnetic field will be eastward near the ICB and westward near the CMB. According to Alfvén's theorem, this winding-up process would continue for as long as the forces driving the motion could maintain it (see below). In reality, however, η is not zero, and the field lines diffuse relative to the moving conductor. Eventually a balance may be established in which the rate at which field lines are drawn out longitudinally by the thermal winds is exactly cancelled by the rate at which they drift in the opposite direction through ohmic diffusion. In short, the total field, the sum of the inducing and induced fields, tends to align itself with the helical streamlines of the total flow, the sum of the meridional and zonal motions.

4. Dynamics; why the magnetic compass needle points North (or South!)

After the initial successes of Herzenberg and Backus, many realistic kinematic geodynamo models were created, realistic in the sense that they operated in spheres with prescribed large-scale fluid motions chosen to incorporate qualitatively the important dynamical effects, as they were perceived at the time. The next step was to include those effects quantitatively by constructing an MHD model of the core, i.e. one that includes the convective dynamics of core flow, and which acts as a dynamo. This is often described as a 'self-consistent dynamo problem', since it includes the back-reaction of the magnetic field on the fluid flow. This is an altogether tougher nut to crack than the kinematic dynamo. It includes the kinematic problem but requires the solution of further equations (see below). Moreover, unlike the kinematic problem, the MHD problem involves nonlinear equations; because of Cowling's theorem, three-dimensional solutions must be sought.

There are two useful ways of looking at the back reaction of the magnetic field on the fluid flow: the Lorentz force, $\mathbf{J} \times \mathbf{B}$ per unit volume, and the Faraday–Maxwell stresses. Their mathematical equivalence follows from the result

$$\mathbf{J} \times \mathbf{B} = \frac{1}{\mu_0}(\nabla \times \mathbf{B}) \times \mathbf{B} = -\nabla\left(\frac{B^2}{2\mu_0}\right) + \nabla \cdot \left(\frac{\mathbf{BB}}{\mu_0}\right).$$

This shows that the Faraday–Maxwell stresses consist of an isotropic 'magnetic pressure', $B^2/2\mu_0$, and a 'magnetic tension', B^2/μ_0, along magnetic field lines. The magnetic pressure can be combined with the kinetic pressure p to create a single total pressure; we consider it no further.

Magnetic tension gives elasticity to the (partially) frozen-in field lines. This is responsible for a second mechanism to halt the production of a zonal field by the thermal wind (section 3). We recall that a 'magnetic flux tube' consists of a bundle of lines of force, i.e. it is a tube, generally curved, whose surface is everywhere parallel to $\mathbf{B}$. If $\eta = 0$, a tube always contains, by Alfvén's theorem, the same fluid particles, the same field lines, and therefore the same flux of field

$$\sum = \int_A \mathbf{B} \cdot \mathbf{dS}$$

where the integral is taken over any cross-section, A, of the

tube; $\sum$ is the 'strength' of the flux tube. The field imparts a tension of

$$\mathcal{T} = \int_A \frac{B^2}{\mu_0}\, dS$$

to the tube that opposes its further lengthening by the fluid flow. If the tube is stretched, its cross-sectional area diminishes by mass conservation and, since $\sum$ is unchanged, B and $\mathcal{T}$ increase. The tension may become so great that it halts further extension of the tube. Stretching of field lines by fluid flow is an important feature of the dynamo process through which kinetic energy of motion is transformed into magnetic energy at the rate necessary to offset the ohmic degradation of magnetic energy into heat.

Volumetrically, the rate at which kinetic energy is transformed into magnetic energy is $\mathbf{J} \cdot (\mathbf{V} \times \mathbf{B})$ or equivalently $-\nabla \cdot (\mathbf{J} \times \mathbf{B})$, the latter form clearly showing the rate of working of the Lorentz force on the fluid flow. When divided by the mass density, ρ, the Lorentz force becomes the acceleration with which the field attempts to accelerate the flow. More significantly, $\mathbf{J} \times \mathbf{B}/\rho$ is the back reaction of the field that brings $\mathbf{V}$ and Rm to their 'marginal' state, in which the solution of (3) and (4) is, on average, steady. This self-regulation is easily understood. If B diminishes, so does the back reaction provided by the Lorentz force, so that V starts to grow. This enhances field creation, through the first term on the right-hand side of (3). As B increases, so does the Lorentz force, which halts and reverses the growth of V until the average state is restored. If instead B becomes above average, the Lorentz force suppresses V, and B begins to diffuse away through the final, ohmic term in (3). This continues until B resumes its average strength. The average levels of B and V are set by the potency of the buoyancy sources.

As already indicated in section 3, the Coriolis force plays an important role in core dynamics. That it is large compared with the inertial force is apparent from the smallness of their (inverse) ratio, the *Rossby number*,

$$\mathrm{Ro} = \frac{V}{2\Omega r_{\mathrm{CMB}}},$$

which is of order 10^{-5}. That it is large compared with viscous forces is clear from the minute size of their (inverse) ratio, the *Ekman number*,

$$E = \frac{\bar{\nu}}{2\Omega r_{\mathrm{CMB}}^2},$$

where ν is the kinematic viscosity. The molecular viscosity of the FOC is sometimes said to be the worst known quantity in geophysics. A value of $\bar{\nu}$ near 10^{-6} m^2 s^{-1} is often adopted, giving $E \approx 10^{-15}$. Even if $\bar{\nu}$ is increased by 10^6 on the grounds that core turbulence enhances momentum transport in the core, E is still only 10^{-9}. It seems clear that the viscosity of the FOC is significant only in boundary layers abutting the CMB and ICB. Apart from the (non-hydrostatic) pressure gradient, the only term comparable with the Coriolis force is the Lorentz force. Obtaining an esimtate of $\mathbf{J}$ from Ohm's law [$\mathbf{J} = \sigma(\mathbf{E} + \mathbf{V} \times \mathbf{B})$], we see that the ratio of Lorentz to Coriolis forces is roughly

$$\Lambda = \frac{\sigma B^2}{2\Omega\rho},$$

which is the *Elsasser number*. The numerical simulations described below suggest that the core operates in a so-called 'strong field regime', in which Λ is O(1) or greater. There is also indirect geophysical support for this. In answer to Q4 and Q5, the buoyancy sources set the level of V, and an approximate balance between the Coriolis and Lorentz forces [$\Lambda =$ O(1)] sets the scale of the field intensity, B, in the core and therefore on the Earth's surface.

The buoyancy force is typically smaller than the Coriolis force, the Lorentz force and the (non-hydrostatic) pressure gradient. It is nevertheless crucially important, since it alone provides the power source for the fluid motions. This depends on the release of heat and light material at the ICB as described in section 2. These sources are combined in a single variable, the co-density C, which will be defined later. The buoyancy force, being parallel to gravity, is radially inwards. Overall, it has no preferred direction in space, and this is true of all the other forces we have considered with the single exception of the Coriolis force, which is therefore able to impress its preferred direction, Ω on the MHD state of the core. This ultimately provides answers to Q6 and Q7: the magnetic compass needle points approximately North–South because of the preferred direction of the Coriolis force. Although other forces, such as the buoyancy and Lorentz forces, have no intrinsically preferred direction, the Coriolis imposes its preferred direction on them because it is potent in determining $\mathbf{V}$, on which they depend.

The theory of convection is generally and conveniently formulated in terms of deviations from a reference state. It is clearly advantageous to adopt the PREM model described in section 2. In this state the entropy $\bar{S}$ per unit mass and the mass fraction of the light constituent of core fluid $\bar{\xi}$ are uniform in the FOC through mixing by the self same convective motions that it is our objective to determine! Since PREM is in hydrostatic equilibrium, variables in the convective state differ only slightly from those in PREM, so that for instance the deviation ρ in density from $\bar{\rho}$ is, to a very good approximation,

$$\rho = \left(\frac{\partial \bar{\rho}}{\partial S}\right)_{\xi,p} S + \left(\frac{\partial \bar{\rho}}{\partial \xi}\right)_{p,S} \xi + \left(\frac{\partial \bar{\rho}}{\partial p}\right)_{S,\xi} p,$$

or

$$\rho = C\bar{\rho} + \left(\frac{\partial \bar{\rho}}{\partial p}\right)_{S,\xi} p,$$

where

$$C = \frac{1}{\rho}\left[\left(\frac{\overline{\partial\rho}}{\partial S}\right)_{\xi,p} S + \left(\frac{\overline{\partial\rho}}{\partial\xi}\right)_{p,S} \xi\right]. \tag{5}$$

Here, as elsewhere below, an unbarred symbol represents the convective contribution to the variable, e.g. the total density is $\overline{\rho} + \rho$. The second form (5) for ρ is convenient, since it separates the effects of p on the convective density, which play no part in the buoyancy mechanism, from those of S and ξ which do, and which are conveniently combined together in the 'co-density', C (Braginsky and Roberts 1995). In an allied simplification, conservation of mass is reduced to satisfying the anelastic equation.

$$\nabla\cdot\overline{\rho}\mathbf{v} = 0 \tag{6}$$

In full, the momentum equation is

$$\overline{\rho}\frac{\partial\mathbf{v}}{\partial t} = -\nabla\cdot(\overline{\rho}\mathbf{v}\mathbf{v}) - 2\overline{\rho}\Omega\times\mathbf{v} - \overline{\rho}\nabla\left(\frac{p}{\overline{\rho}} + U\right) - C\overline{\rho g}\hat{\mathbf{r}}$$
$$+\nabla\cdot\left[2\overline{\rho\nu}\left(\overleftrightarrow{e} - \frac{1}{3}(\nabla\cdot\mathbf{v})\overleftrightarrow{\delta}\right)\right] + \frac{1}{\mu_0}(\nabla\times\mathbf{B})\times\mathbf{B}. \tag{7}$$

Here $C\overline{\rho g}\hat{\mathbf{r}}$ is the buoyancy force, $\hat{\mathbf{r}}$ is the radial unit vector, and $\overline{g}$ is the acceleration due to gravity in the reference state; U is the change in gravitational potential brought about by the density differences ρ associated with convection; $\mathbf{B}$ and $\mathbf{v}$ can be obtained without determining U, but if necessary U can be derived from Newtonian gravitation theory, by solving $\nabla^2 U = 4\pi G\rho$; $\mathbf{v}$ and $\mathbf{B}$ are the large-scale parts of the velocity and magnetic fields that are numerically resolvable; the effect of the small scale parts on these large scale fields is regarded as satisfactorily represented by replacing molecular diffusivities by turbulent diffusivities. The term $\overline{\rho\nu}\left(\overleftrightarrow{e} - \frac{1}{3}(\nabla\cdot\mathbf{v})\overleftrightarrow{\delta}\right)$ represents the viscous stresses, which are weak except in boundary layers; $\overleftrightarrow{e}$ is the rate of strain tensor $[e_{ij} = \frac{1}{2}(\nabla_i v_j + \nabla_j v_i)]$, $\overleftrightarrow{\delta}$ is the identity tensor and $\overline{\nu}$ is the kinematic (turbulent) viscosity. Since Ro $\ll 1$, the inertial terms $\overline{\rho}\partial\mathbf{v}/\partial t$ and $-\nabla\cdot(\overline{\rho}\mathbf{v}\mathbf{v})$ are both very small compared with other contributions to (7). We retain only their largest parts, which are axisymmetric and zonal. We do this to add a little more geophysical realism; their effect on the solutions is slight. They are associated with torsional waves in the core, which are described briefly below and for which there is some observational evidence. In the reference frame in which (7) is written, the angular momentum of the Earth is zero. The angular velocity Ω of the frame is almost the same as that of the mantle, but the mantle moves relative to the reference frame, in response to the viscous and magnetic stresses to which the core subjects it. The magnetic stresses create a non-zero torque on the mantle because, to simulate crudely the D″ layer (a thin region at the bottom of the mantle, identified seismologically, and thought to be an inhomogeneous thermal boundary layer that is almost certainly more highly conducting than the rest of the mantle), we added a thin layer of good electrical conductor at the base of the mantle. Its radially integrated conductivity has an Earth-like value of 4×10^6 S in our models. The viscous and magnetic stresses produce variations in the rotation period of the mantle that have roughly the same magnitude and temporal variation as the observed decade variations in length of day.

The co-density C arises through the slow evolution of the reference state, which provides sources of S and ξ at the ICB and volumetric sinks represented by the final terms in the governing equations below, in which the overdot denotes the rate of change on the geological time scale on which the Earth cools and the core grows:

$$\overline{\rho}\frac{\partial S}{\partial t} = -\nabla\cdot(\overline{\rho}S\mathbf{v}) + \nabla\cdot(\overline{\rho\kappa}^S\nabla S) + \frac{1}{\overline{T}r^2}\frac{\mathrm{d}}{\mathrm{d}r}\left(C_p\overline{\rho\kappa}^T r^2\frac{d\overline{T}}{\mathrm{d}r}\right)$$
$$+\frac{\overline{\eta}}{\mu_0\overline{T}}\left|\nabla\times\mathbf{B}\right|^2 + \frac{\overline{g}}{\overline{T}}\left[\overline{\kappa}^S\left(\frac{\overline{\partial\rho}}{\partial S}\right)_{\xi,p}\frac{\partial S}{\partial r} + \overline{\kappa}^\xi\left(\frac{\overline{\partial\rho}}{\partial\xi}\right)_{S,p}\frac{\partial\xi}{\partial r}\right] - \overline{\rho}\dot{\overline{S}}, \tag{8}$$

$$\overline{\rho}\frac{\partial\xi}{\partial t} = -\nabla\cdot(\overline{\rho}\xi\mathbf{v}) + \nabla\cdot(\overline{\rho\kappa}^\xi\nabla\xi) - \overline{\rho}\dot{\overline{\xi}} \tag{9}$$

The first terms on the right-hand sides of (8) and (9) represent the advection of S and ξ by the convective motions. The following terms represent the diffusion of these quantities, mainly by small-scale turbulence, the corresponding diffusivities, $\overline{\kappa}^S$ and $\overline{\kappa}^\xi$, are therefore likely to be almost the same. The third term on the right-hand side of (8) describes entropy transport in the reference state, $\overline{\kappa}^T$ being the thermal conductivity. The fourth and fifth terms recognize the creation of entropy by ohmic dissipation, and by the diffusion of entropy and composition. The sources of S and ξ lie mainly, however, on the ICB, and are proportional to the rate of freezing and therefore to each other. Heat conduction removes entropy, but there is no corresponding flux of ξ into the mantle. According to current geochemical thinking, there is essentially no radioactivity in the core, and no such heat sources are included in (8). The core dynamo is driven *entirely* by the secular cooling of the Earth and the concomitant buoyancy release at the ICB as the SIC freezes.

It is easily verified that (3)–(9) and the associated boundary conditions are invariant under a transformation in which $\mathbf{B}(\mathbf{x},t) \to -\mathbf{B}(\mathbf{x},t)$, all other variables ($\mathbf{v}$, p, S, ξ, etc) being unchanged. This answers Q11: a homogeneous dynamo has no preference for one field polarity over the other.

It is appropriate to make a few remarks about the time scales of core MHD. We first return to the flux tube described earlier, which resembles an elastic string in tension $\mathcal{T}$, its mass per unit length being

$$\mathcal{M} = \int_A \rho \, \mathrm{d}S.$$

Alfvén argues that, like the string, the tube can transmit disturbances along it with a wave speed $(\mathcal{T}/\mathcal{M})^{1/2}$ which, in the limit of a tube of small cross-section A, is the *Alfvén velocity*

$$V_\mathrm{A} = \frac{B}{(\mu_0 \rho)^{1/2}}. \tag{10}$$

Such transverse waves are called *Alfvén waves* or *hydromagnetic waves*. They rely on the inertial force which, as we have seen, is generally much smaller than the Coriolis force. This means that (10) is largely irrelevant in core dynamics, its place being taken by the much slower wave speed

$$V_\mathrm{s} = \frac{V_\mathrm{A}^2}{2\Omega r_\mathrm{CMB}} = \frac{B^2}{2\Omega \mu_0 \rho r_\mathrm{CMB}}.$$

The corresponding time scale, $\tau_\mathrm{s} = r_\mathrm{CMB}/V_\mathrm{s}$, is of centuries or more, which is suggestive of the secular variation.

An exception is the torsional wave, which travels across the core, towards and away from the rotation axis. The fluid on each cylinder coaxial with O_z turns about O_z relative to its neighbours and is magnetically coupled to them. The Coriolis force on such a motion can be almost completely balanced by the kinetic pressure and is therefore dynamically ineffective. The inertial force again becomes influential and, as a result, torsional waves are much the same as Alfvén waves. They cross the core in a time $r_\mathrm{CMB}/V_\mathrm{A}$ that is measured in years or at most a few decades. We do not have space in this article to describe torsional waves further.

Other time scales significant in core MHD include the diffusion time τ_σ introduced in section 1, and the overturning time of the convection $\tau_V = (r_\mathrm{CMB} - r_\mathrm{ICB})/V$ based on a typical speed V of convective motions. In our simulations, τ_V is at most a few hundred years, and is therefore of much the same order as τ_s. This may in fact explain why (see Q13) the westward drift appears in our simulations partially as a wave phenomenon and partially as a convective phenomenon; see section 7.

5. How the inner core affects core MHD; an electric motor in the core

At first it seems to have been generally felt that the SIC plays no essential role in core MHD, and could be dispensed with entirely without significant loss of geophysical realism. The buoyancy sources at the ICB that supply power to the dynamo could be replaced by volumetric heat sources spread throughout the fluid. If the SIC was recognized at all, it was retained for numerical reasons, to evade possible difficulties with the coordinate singularity that arises in the obviously convenient, spherical coordinate system (r, θ, ϕ), where θ is co-latitude, and ϕ is longitude. Usually, when the inner core was included, it was for simplicity assumed to be a perfect electrical conductor or an electrical insulator, although neither of these extremes is true; the SIC has much the same conductivity as the FOC. To a large degree, this cavalier treatment of the SIC was forced on theorists by the computing environment of the 1960s and 1970s. It was defended on the grounds that the SIC is only 5% of the core by mass and 4% by volume. Surely such a small body can do little to influence the fluid dynamo?

It has become apparent over the past decade that the SIC is surprisingly important from at least two points of view. First, the ohmic diffusion time of the SIC is of the order of 1–2 thousand years. The magnetic field threading the SIC cannot dramatically change its direction or magnitude in a much shorter time than this. The time scale, τ_V, on which the magnetic and convective velocity fields in the FOC change is significantly less, at most a few hundred years. As Hollerbach and Jones (1993a,b) recognized, this means that the inner core moderates the MHD of the FOC, a fact that we subsequently confirmed (see section 7). Second, because of the large Coriolis force, the SIC creates a *Taylor column* in the core. In its simplest form, a Taylor column arises when the main forces acting on a fluid are the Coriolis force and the pressure gradient; the viscous force is assumed small ($E \ll 1$), the buoyancy and magnetic forces are absent, and if the motions are slow ($\mathrm{Ro} \ll 1$) the inertial forces are negligible. G.I. Taylor demonstrated both theoretically and experimentally that, when a solid object moves through the fluid in these conditions, it carries with it the contents of a cylinder whose surface circumscribes the body and is everywhere parallel to Ω. The SIC defines such a Taylor column. Its surface, $\mathcal{C}$, is called 'the tangent cylinder'. It is parallel to O_z and touches the ICB on its equator, so that its radius is r_ICB; see figure 2. The dynamics of the exterior $\mathcal{E}$ of the cylinder are largely disconnected from the dynamics of its interior $\mathcal{I}$. For example, if the SIC rotates with an angular velocity slightly different from the mantle, the fluid in $\mathcal{E}$ co-rotates with the mantle, but the fluid in $\mathcal{I}$ rotates with an angular velocity midway between those of mantle and SIC. The fluid in $\mathcal{I}$ lies in two separate regions, $\mathcal{N}$ and $\mathcal{S}$, North and South of the ICB. These are weakly linked dynamically through the SIC lying between them. Although it might seem that this dichotomy (or trichotomy) does not apply to the FOC, in which the Lorentz force is strong and the buoyancy force is significant, this is not necessarily so, as Hollerbach (1994) first recognized, and we have confirmed this. We have found that the MHD states of $\mathcal{N}$ and $\mathcal{S}$ are far more active dynamically than is that of $\mathcal{E}$.

A state in which the SIC does not co-rotate with the lower fluid core does not last long. Suppose for example that its angular velocity, Ω_SIC, is initially zero, and that the

predominantly S→N meridional circulation sketched in figure 2 exists in $\mathcal{N}$. We have seen in section 3 that Coriolis forces then create a zonal thermal wind that is eastwards just above the ICB, and that this adds an eastward zonal component to a meridional field in the S→N direction. The lines of the total field are deflected zonally and, acting like elastic strings, they drag the SIC in the eastward direction. The SIC responds by accelerating in the same sense. The Coriolis force acting on the motion in $\mathcal{S}$ also creates an eastward thermal wind just above the ICB that induces from the S→N field a westward field that re-enforces the couple exerted by $\mathcal{N}$ on the SIC. Once these couples have increased the eastward velocity, $\Omega_{\rm SIC} r \sin\theta$, of the SIC to the appropriate average of V_ϕ just above the ICB, the elastic strings pull equally in both the E→W and W→E directions, and the net magnetic couple on the SIC becomes zero (even though the magnetic stresses on the surface of the ICB remain large locally). The process may be regarded as an example of Lenz's Law or of Le Chatelier's Principle. One may also picture the SIC as the rotor of a synchronous electric motor, driven into rotation by dynamo-created electric currents. It is of course impossible to predict which way the motor will turn until (3)–(9) have been solved, and the existence of motions similar to those postulated in figure 2 has been established. Before this can be done, further boundary conditions must be specified. These conditions are very significant.

6. Core–mantle interactions

The boundary conditions at the ICB constrain the local flux of the heat of crystallization to be proportional to the flux of light constituent and to the local cooling rate; the constants of proportionality depend on physical properites of core material some of which are poorly determined. This is not to be wondered at, bearing in mind that it is not even known what the predominant light constituent of core fluid is! The boundary condition on the heat flux, $\mathcal{Q}$, at the CMB controls the cooling rate of the core and therefore the buoyancy sources at the ICB, the vigour of convection and the intensity of the magnetic field. The heat flux is not well known, and we had to rely for guidance on recent simulations of mantle convection by Tackley *et al.* (1994). We specified $\mathcal{Q} = 7\cdot2$ TW, and we supposed initially that this is uniformly distributed over the CMB. The resulting time-averaged growth rate of $r_{\rm ICB}$ is about 10^{-11} m s^{-1}, or 3 cm/century. If $\mathcal{Q}$ had this value over its entire lifetime, the age of the SIC would be roughly one billion years, less than a quarter of the age of the Earth. In later simulations, some of the results from which are published here for the first time, we conducted three further numerical experiments. The motivations and definitions of these models are the following.

We shall call our first simulation, briefly described above, 'model 1'. Model 2 was motivated by the ever-strengthening evidence from seismic tomography that significant lateral inhomogeneities exist in the mantle. These are usually interpreted as being due to horizontal variations in temperature, probably associated with global convection in the mantle. As a result of these, the heat flux, $F(\theta,\phi,t)$, per unit area out of the core through the CMB necessarily varies with co-latitude θ, longitude ϕ, and time t, though it is still not known how strongly. We write

$$F(\theta,\phi,t) = \overline{F}(t) + k_1 f(\theta,\phi,t), \tag{11}$$

where f has a zero horizontal average and k_1 is a constant. Virtually nothing is yet known with certainty about $\overline{F}$, k_1 and f. All that can be said with confidence is that, since the time scales for mantle convection are a million times longer than those of core convection, we are justified in assuming that, for the duration of our simulations, F is time-independent in the reference frame moving with the mantle. It follows that $\overline{F}$ is constant, and that f depends on t in a way that can be (and was) predicted by the angular velocity of the mantle with respect to our reference frame. Somewhat abitrarily, we assume that f is proportional to the present day structure of the seismic heterogeneities in the lower mantle as determined by Su and Dziewonski (1995); see figure 3. The constant $\overline{F}$ in (11) is chosen to be $\mathcal{Q}/4\pi r_{\rm CMB}^2$, so that the net heat flux

$$\mathcal{Q} = \int_{\rm CMB} F(\theta,\phi,t)\,{\rm d}S, \tag{12}$$

is the assigned $\mathcal{Q}$, for which model 2 is again 7·2 TW. This makes it, like model 1, superadiabatic at the CMB. Again somewhat arbitrarily, the constant k_1 selected for model 2

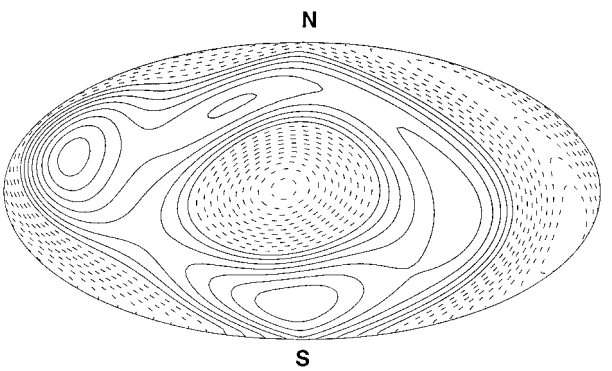

Figure 3. A snapshot of the function $f(\theta,\phi,t)$ that defines the non-uniform heat flux from the core to the mantle; (see 11). Here θ is co-latitude and ϕ is longitude. Solid contours represent outward heat flux larger than the mean; broken contours represent heat flux smaller than the mean, and possibly inward. The entire spherical surface is plotted in this equal area projection; the North pole is at centre-top; the South pole is at centre-bottom; the equator is a straight horizontal line through the centre of the projection.

makes the maximum variation in the local heat flux (relative to the mean heat flux) greater than the mean superadiabatic heat flux at the CMB by a factor of 3. Some simulations of mantle convection find this factor to be as high as 10 (Tackley *et al.* 1994).

Models 3 and 4 were motivated by the fact that, in principle, core convection can pump heat inwards at the CMB (Loper 1978). In essence, the compositional buoyancy is then so great that it controls the thermal buoyancy and the outward heat flux. In such a subadiabatic model, the upper layers of the FOC are stably stratified, and there is some indirect evidence that this may be the case. The geophysical implications of a stable upper core have been considered by Braginsky (1993). Because of the compositional source at the ICB, the lower core is gravitationally unstable and convects; there is no obvious reason why it should not operate a dynamo. In models 3 and 4, we suppose that $\mathcal{Q} = 3$ TW which is 2 TW less than what an adiabatic temperature gradient would conduct from the core. In model 3 it is assumed that $\mathcal{Q}$ is uniformly distributed over the CMB (i.e. $k_1 = 0$) but k_1 is chosen in model 4 so that the maximum variation in the local heat flux (relative to the mean) is about 3 times the mean subadiabatic heat flux at the CMB).

Apart from these differences in heat flux conditions, there are absolutely no differences in the specifications of our four models. We shall focus on them in section 8, but first briefly review a preliminary model (Glatzmaier and Roberts 1995a, b, 1996c) which we shall call 'model 0', in which the reference state is homogeneous, i.e. $\overline{\rho}$ is spatially uniform. The comparative simplicity of such 'Boussinesq' models has made them commonplace in convection theory; see, for example, Chandrasekhar (1961).

7. Preliminary numerical experiments: the homogeneous (Boussinesq) model 0

Model 0 is thermally driven; $\overline{\xi}$ and ξ play no role, and $\overline{T}$ and T replace $\overline{S}$ and S. Buoyancy is supplied by a uniform heat flux, $\mathcal{Q}$, at the ICB, with the CMB held at constant temperature. In an attempt to compensate for the lack of compositional buoyancy, thermal buoyancy was deliberately though artificially increased by taking $\mathcal{Q} = 50$ TW. We suggest below that this level of compensation may have been somewhat too great.

Equations (3)–(9) were solved using a spectral method (spherical harmonic and Chebyshev polynomial expansions) that treats all linear terms implicitly and nonlinear terms explicitly (Glatzmaier 1984, Glatzmaier and Roberts 1995a). The integration time step was typically 20 days. Our aim in choosing the defining parameters of all 5 models was first and foremost that we should not contradict any incontrovertible geophysical fact, such as the angular velocity of the Earth and the physical dimensions of the inner and outer cores. In models 1–4, we made the reference state agree closely with PREM. With the exception of $\overline{\nu}$, the values of other parameters that are less well known were generally taken from Braginsky and Roberts (1995) and are not discordant with any geophysical data known to us. But for numerical reasons we could make $\overline{\nu}$ no smaller than 10^3 m^2 s^{-1}, which is greater by at least three orders of magnitude than plausible estimates of even the turbulent viscosity. Nevertheless, the corresponding Ekman number, E, is small ($\sim 10^{-6}$), and this indicates that viscous forces are insignificant in the bulk of the FOC. We could in fact show that their effect is prinicpally confined to boundary layers at the ICB and CMB. We established that, compared with magnetic stresses, viscous stresses on the ICB are, as for the real Earth, negligible in our models. Viscous coupling at the CMB does, however, influence the changes in the length of day in our models, when in reality it very probably does not (e.g. Roberts 1989). Small differences in mantle rotation have little effect on core dynamics, and it seems to us that even a viscosity as large as the one we were compelled to adopt should have almost no effect on the dynamics of the FOC or SIC.

Model 0 was integrated for about 40 000 years of simulated time (Glatzmaier and Roberts 1995a, b). The starting point was a random temperature perturbation and a random 'seed' field, without which a magnetic field would not be generated (since $\mathbf{B} \equiv 0$ satisfies all equations and boundary conditions). After approximately 15 000 years, the solution appears to lose 'memory' of its initial state, and to enter a strongly varying regime that (apart from one interlude described below) is statistically steady. The dipole moment, $\mathbf{m}$, of the field is then typically within $10^\circ - 20^\circ$ of the geographic axis and its magnitude $m = |\mathbf{m}|$ is typically 20×10^{22} A m^2. Since this regime persists for the duration of the integration, that is for about twice τ_σ, we may fairly claim that the model is a self-excited dynamo. Based on the intensity of the geomagnetic field outside the core and the fluid flow inferred from the westward drift of the geomagnetic field, it has for many years been widely believed that the energy, $\mathcal{M}$, of the geomagnetic field is large compared with the kinetic energy, $\mathcal{K}$, of core flow, as measured in the rotating frame. In this and simulations 1 and 2 below, $\mathcal{M}$ is typically three orders of magnitude greater than $\mathcal{K}$ (but in simulation 4, $\mathcal{M}/\mathcal{K} \approx \frac{1}{4}$).

Different convective regimes exist inside and outside the tangent cylinder, $\mathcal{C}$, principally because the rotation vector, Ω, is mainly parallel (perpendicular) to $\overline{g}$ inside (outside) the tangent cylinder. It has long been recognized that heat is more efficiently removed from a rapidly rotating body of fluid, such as the Earth's core, by non-axisymmetric motions outside the tangent cylinder that carry heat away from the axis of rotation than by nearly axisymmetric motions inside the tangent cylinder that transport heat toward the poles. In fact, convection in $\mathcal{E}$ carries heat so

4a

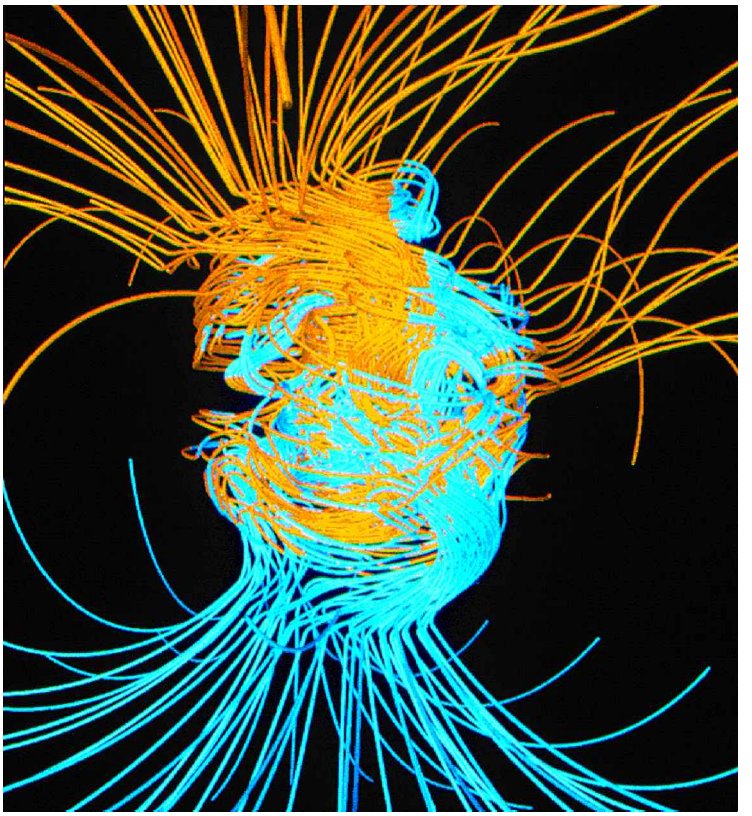

4b

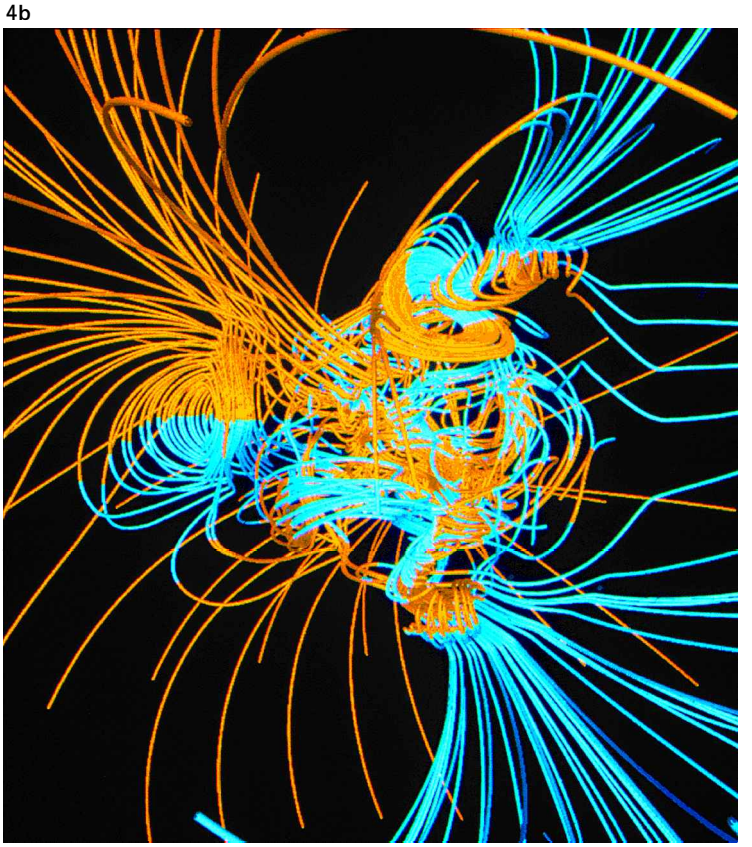

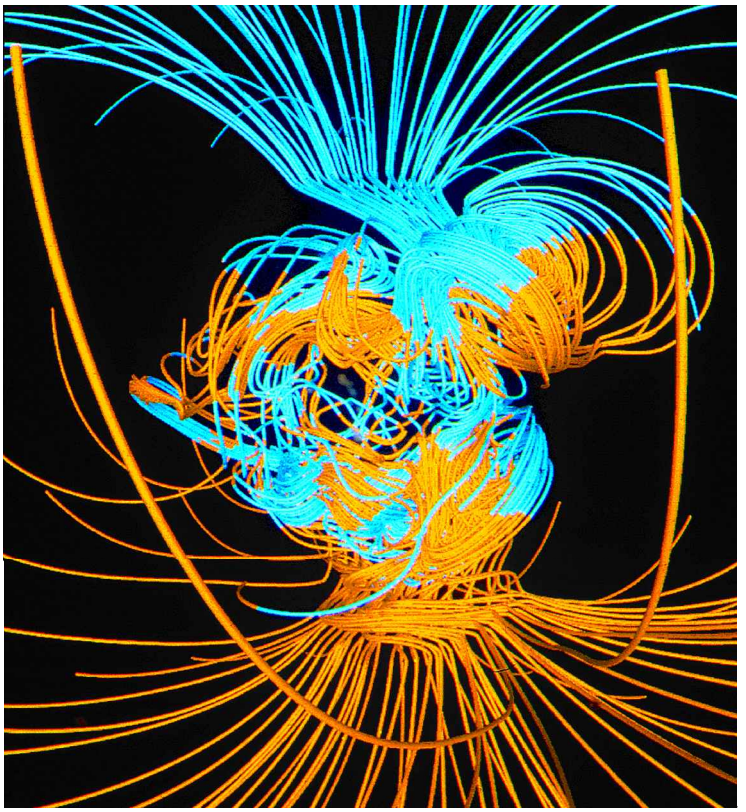

Figure 4. The three-dimensional magnetic field of model 0, portrayed through its field lines (*a*) before the reversal, (*b*) mid-way through the transition, and (*c*) after the reversal. The sequence spans 2000 years. The North (South) geographic pole is at the top (bottom) of each plot. Lines are coloured gold (blue) when the radial component of the field is directed outward (inward).

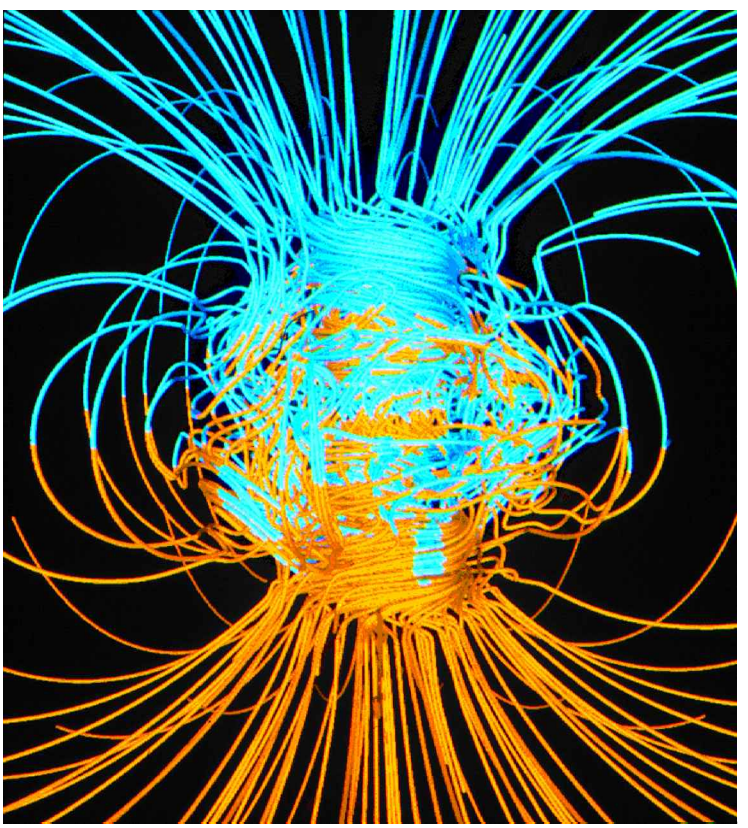

Figure 6. A snapshot of the three-dimensional magnetic field in the variant of model 0 in which the viscosity of the FOC is everywhere the same, i.e. is not enhanced near the core–mantle boundary, as it was in model 0 itself. The field is portrayed via lines of force that are plotted out to two Earth radii. Gold (blue) lines represent outwardly (inwardly) directed magnetic field. The rotation axis is vertical. The transition at the core–mantle boundary from the smooth, external potential field to the more intense, complicated field inside the core is worthy of note.

efficiently that the whole of that volume is nearly isothermal, apart from a thermal boundary layer at the CMB. In $\mathcal{I}$, however, heat is convected less effectively, and additional buoyancy develops through a temperature difference between $\mathcal{I}$ and $\mathcal{E}$ The buoyancy force produces an outward flow along the rotation axis, in the way envisaged in section 3 and sketched in figure 2. As anticipated in that section, Coriolis forces create a thermal wind that is eastward near the ICB and a westward near the CMB, and the meridional field is sheared in the zonal direction, to the East near the ICB and to the West near the CMB. The outward motions near the CMB tend to twist the zonal fields back into the meridional direction, and out into the mantle, so maintaining the meridional field and giving it an axial dipole dominance, i.e. producing a dipolar field nearly aligned with the rotation axis. The non-dipolar part of the simulated field at the CMB is qualitatively similar in structure to the Earth's. Also like the Earth, it features drift westward at roughly $0{\cdot}2^\circ$/yr. This motion is partly phase propagation and partly due to a weak westward flow beneath the CMB and outside the tangent cylinder.

The existence of an eastward thermal wind near the ICB implies, for the reasons given in section 5, that the inner core also moves eastward. Based on model 0, we predicted that the rotation rate of the inner core, Ω_{SIC}, would exceed that of the mantle by 1°–3° per year (Glatzmaier and Roberts, 1995a). This prediction has now been supported by two independent analyses of seismic data: first that of Song and Richards (1996) who estimated 1°/yr and then that of Su *et al.* (1996), who estimated 3°/yr, both eastward relative to the mantle, as in our simulation. We describe this further in section 8.1 below.

One of the striking features of model 0 (and model 2 below) is its stochasticity. Several times during the integration, the magnetic field generated in the FOC seemed to be trying to reverse, but without success. On each occasion, the field threading the inner core, which can change significantly only on a time scale of order 10^3 years (see section 5), maintained itself strongly enough to outlast the reversal attempt, and then helped to reinstate the original field directions in the core. During one episode (about 36 000 years into the simulation), however, the field in the FOC maintained a reversed direction adjacent to the ICB for such a long time that it could diffuse into the SIC and replace the pre-existing field there by a field in the opposite direction. After that, the reversed state became established in the FOC also. This process, which was accompanied by reductions in m and $\mathcal{M}$ of about 80% and by a temporary reversal in the sense of inner core rotation, was the interlude referred to above. For the first time to our knowledge, a geomagnetic field reversal had been simulated by a realistic dynamo model. The reversal took a little more than a thousand years to complete, and after it was over the system returned to a state that was indistinguishable from the pre-reversal state, except for the oppositely directed magnetic field. Although several further abortive reversals occurred, none were successful during the remaining time over which the model was integrated. Field lines are shown in figure 4 before, during and after the reversal. The time spanned by the sequence is 2000 years and the centre picture shows the field at the mid-point of the reversal, defined as the instant at which the dipole moment of the solution as seen on the CMB is equatorial (**m** perpendicular to Ω).

In some respects, the reversal seemed quite similar to those that have been analysed for the Earth (see Q9). Paleomagnetists usually describe their findings in terms of the virtual geomagnetic poles and virtual dipole moments defined in section 1. As noted there, VGPs and VDMs differ from the true geomagnetic poles and true dipole moment. We extracted from our solution the paths of the VGPs during the reversal at several hypothetical collection sites. Apart from the fact that they all start near one geographic pole and finish near the other, these paths show little resemblance to one another or to the corresponding path of the TGP; the paths of the VGPs are considerably more tortuous than that of the TGP (Glatzmaier and Roberts, 1995b). Similarly, although the VDMs and TDM display the same temporary decrease during the reversal, the VDMs show a much greater variability than the TDM, which is shown in figure 5. At the mid-point of the reversal, m is $1{\cdot}6 \times 10^{22}$ A m^2, or about 10% of the typical value of the TDM before and after the reversal; the typical VDM at mid-reversal for the real Earth is roughly 25% of the present day dipole moment.

We noted above that, to compensate for the lack of compositional buoyancy, we had to increase the thermal

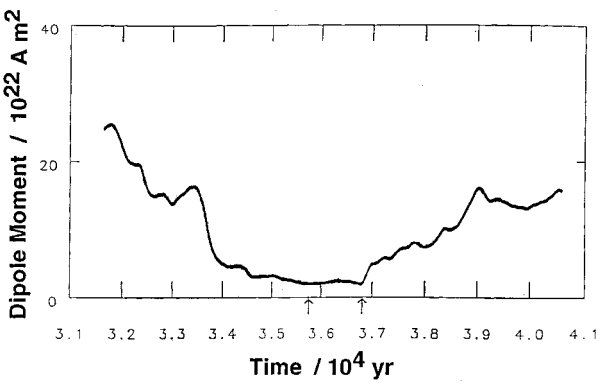

Figure 5. The true dipole moment, *m*, during 9000 years spanning the polarity reversal of model 0. The times indicated are from the beginning of our simulation. The first arrow marks the mid-point in the transition as seen at the inner core boundary and the second marks the mid-point as seen at the Earth's surface. (After Glatzmaier and Roberts (1995b).)

driving in model 0 above the 7.2 TW heat flux assumed in models 1 and 2. There are, however, several indications that we overcompensated, i.e. the heat flux $\mathcal{Q}$ that we selected was somewhat too large for geophysical realism. For example, m is typically more than twice that of the present day Earth, the reversal is complete in 1200 years rather than in the 3000 – 5000 years suggested by the paleomagnetic data, and the reversal occurs comparatively soon after the simulation was started, rather than after a time of order 200 000 years or greater, as paleomagnetic research indicates. The integrations are, however, computationally intensive, and the 40 000 years of simulated time over which model 0 was integrated expended over 2000 hours of Cray C90 time. The luxury of experimenting with many different input parameters is not available to us. And we also believe that the general features of the solution described above would not be qualitatively changed by a modest reduction in $\mathcal{Q}$.

Although the reversal mechanism remains elusive in detail, it may in a general sense be a not too surprising behaviour for an MHD system as highly stochastic as model 0, which was driven significantly harder than necessary for it to function as a dynamo. This answer to Q8 is however perhaps a little glib. During numerical experiments to determine what effect different defining parameters would have on the solution, we found that one particular change had significant consequences. In an effort to simulate the effects of topographic coupling between core and mantle, we had artificially enhanced the viscosity in the uppermost 230 km of the core. When we removed this feature from model 0, the character of the solution changed markedly. It became more strongly dipolar, as can be seen by comparing its lines of force, shown in figure 6, with those plotted in figures 4 (*a*) and (*c*). The solution was also much steadier in time; it showed no tendency to reverse in the remaining time of roughly 10 000 years during which it was integrated (Glatzmaier and Roberts 1996c). Possibly such a solution is more typical of the geomagnetic field between reversals, but it is still unclear why the system is so sensitive to the viscosity near the CMB.

8. More sophisticated numerical experiments; the inhomogeneous (anelastic) models 1 – 4

8.1. *Model 1*

We now report on our integrations (Glatzmaier and Roberts 1996a, b) of the first of the inhomogeneous, evolutionary models, in which the temperature gradient at the CMB is superadiabatic and independent of θ and ϕ. The associated heat loss across the CMB cools the core and generates thermal and compositional sources at the ICB, both of which are proportional to the local rate at which the ICB advances through freezing. They are therefore proportional to one another. Moreover, S and ξ are advected and diffused in the same way ($\overline{\kappa}^S = \overline{\kappa}^\xi$). Probably for these reasons, we found that the spatial structures of S and ξ are quite similar everywhere in the FOC, except near the CMB, where differences are inevitable; $\nabla_r \xi$ is zero on the CMB because there is no flux of light constituent into the mantle, but $\nabla_r S$ is non-zero, because conduction carries heat into or out of the mantle. Nevertheless, the behaviour of S and ξ elsewhere suggests that the assumption often made by earlier modellers, and by ourselves in model 0, that thermal driving alone adequately describes both types of buoyancy, is not ridiculous.

The ICB is not a perfect sphere; since the SIC rotates at roughly the same angular velocity as the Earth as a whole, it is flattened by centrifugal forces. The resulting equatorial

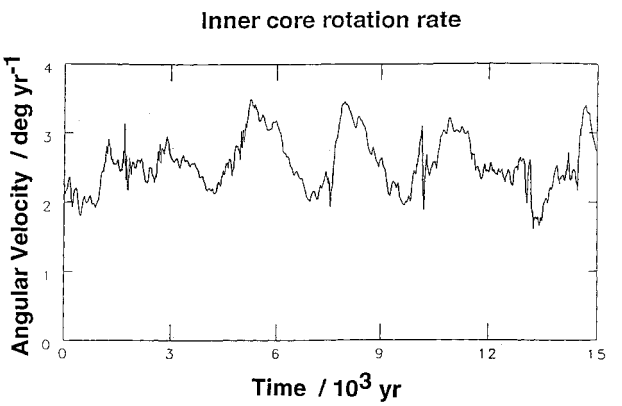

Figure 7. The angular velocity of the inner core, Ω_{SIC}, for a 15 000 year span within the model 1 simulation. (After Glatzmaier and Roberts (1996b).)

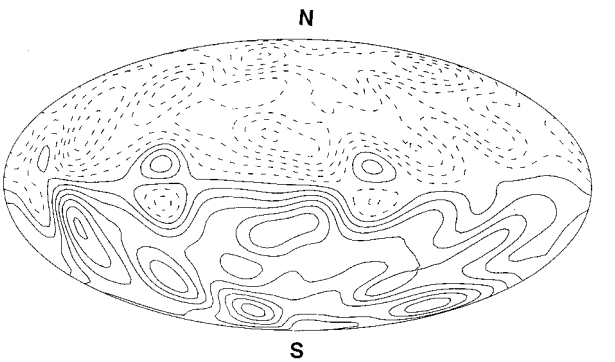

Figure 8. A snapshot of the radial component of the magnetic field produced by model 1 at the core – mantle boundary (equal area projection). The North (South) geographic pole is at the top (bottom) of the projection, the equator being a horizontal line through the middle. The field is directed outward (inward) on the solid (broken) contours. The maximum field intensity outward is 0·24 mT and inward is 0·21 mT.

bulge (the difference between the equatorial and polar radii of the ICB) has been estimated as about 3 km (Mathews *et al.* 1991). Also, Buffett (1996) notes that the inhomogeneities in mass distribution in the mantle distort the surfaces of constant gravitational potential within the core. As a result, the conditions for phase equilibrium that define the surface of the inner core are met at varying distances from the geocentre. He esimates that for this reason the otherwise spheroidal shape of the inner core surface could be distorted by as much as 100 m. In addition to these two effects, a further addition, $h(\theta, \phi, t)$, to the surface topography arises because the sources of buoyancy on the ICB, which are determined by the convection pattern, are not uniform over the ICB. Where the cold convection currents descend onto the ICB, the rate of freezing is enhanced; where the hot rising flows are initiated, the rate of advance of the ICB is diminished. The spatial and temporal form of h has been described by us elsewhere (Glatzmaier and Roberts 1997). It does not exceed 14 m, which is small compared with the 3 km equatorial bulge.

Because of the interest generated by our prediction of inner core super-rotation and its subsequent confirmation by Song and Richards (1996) and Su *et al.* (1996), we investigated the coupling of the inner and outer cores in more detail. We found (Glatzmaier and Roberts 1996b) that the viscous torque on the SIC is usually in the opposite

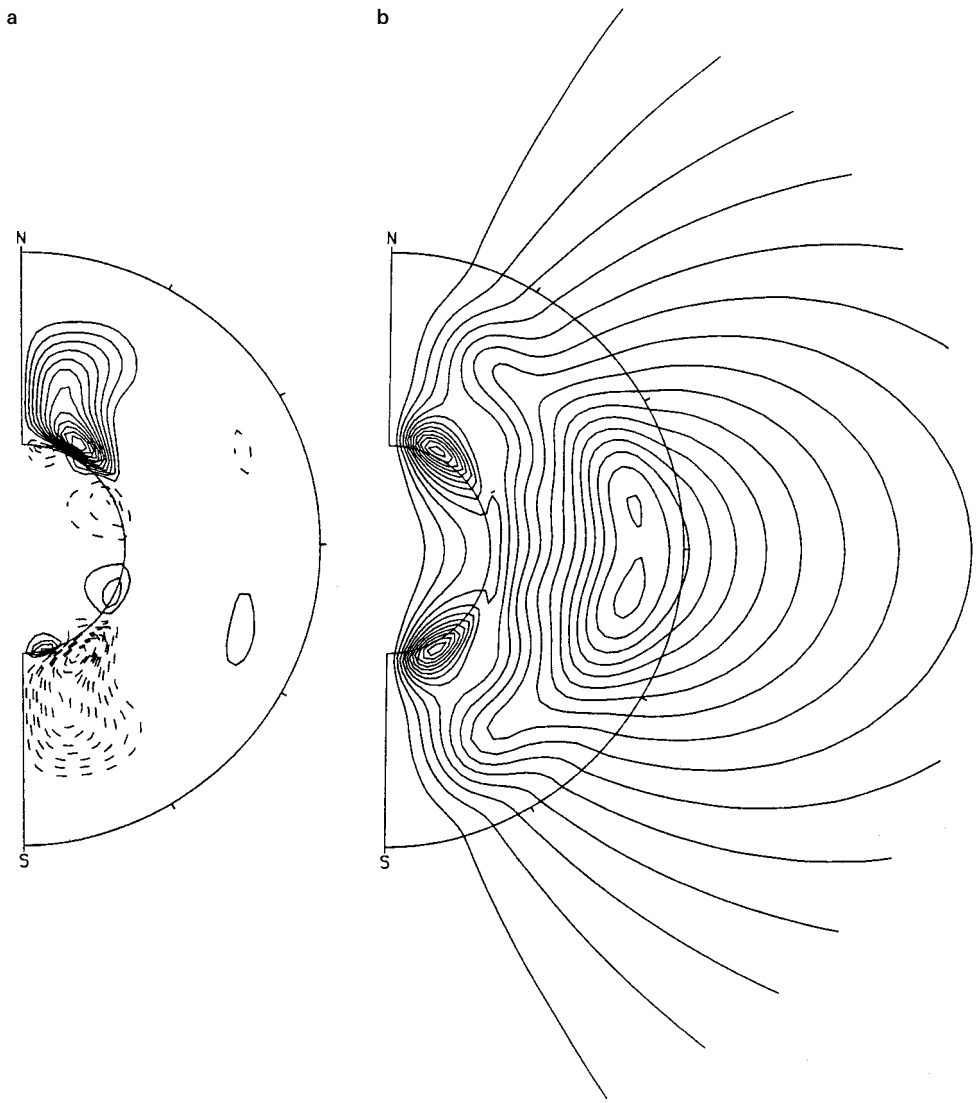

Figure 9. The longitudinal average of the three-dimensional magnetic field typically produced by model 1: (*a*) contours of the zonal field which has a maximum eastward component (shown by the solid curves) of 12 mT and a maximum westward component (shown by the broken curves) of 13 mT; (*b*) lines of force of the meridional field, which is directed counter-clockwise and has a maximum intensity of 18 mT.

direction to the magnetic torque. This accounts for the behaviour of model 0 during the reversal, when the SIC rotated westward for a brief period. The net torque on the SIC is relatively small, oscillating about zero, so maintaining an Ω_{SIC} that is relatively constant on the time scale of decades. The inner core rotation rate for a 15 000 year span of our simulation is shown in figure 7; the average Ω_{SIC} is 2·6°/yr eastward relative to the mantle.

Over the 150 000 years during which it was integrated (starting from the 50 000-year point of model 0), model 1 showed no tendency to reverse its polarity. It was even more dipole-dominated than model 0, so that (for example) the magnetic equator, as seen in figure 8, where the contours of B_r on the CMB are shown, remains in the vicinity of the geographic equator. In fact, figure 8 is strongly reminiscent of similar plots constructed for the present day Earth by Bloxham and Gubbins (1985) and Bloxham and Jackson (1992). Like model 0 and the real Earth, the field patterns show a tendency, more pronounced in some regions than others, to drift westwards.

A typical snapshot of the axisymmetric part of **B** is shown in figure 9, the contours of equal zonal field being displayed in (*a*) and the lines of force of the meridional field in (**b**). It is immediately apparent that, as in model 0, the MHD regimes inside and outside the tangent cylinder C are quite different, and that the intense magnetic activity is confined to the interior I of the cylinder. This stands in sharp contrast with the model recently reported by Kuang and Bloxham (1996) in which the exterior E of the cylinder is dynamically more significant than I. As a result, there is no marked tendency in their solution for the inner core to rotate faster than the mantle or to turn eastward rather than westward relative to the mantle. We attribute this contradiction between their model and ours to differences in the defnining parameters (e.g. rotation rate, heat flux, viscosity, ...) and boundary conditions. It seems to us that the resolution of such disagreements has initiated an exciting new branch of geophysics, that of finding something about the MHD of the deep core from seismology.

8.2. *Model 2*

Considered as a whole, this inhomogeneous model, which has been integrated for more than 100 000 years, is again superadiabatic but, because the heat flux $F(\theta,\phi,t)$ varies strongly over the CMB, there are areas on the CMB where the convective heat flux is inward. The net heat flux, the sum of the adiabatic and convective fluxes, is however everywhere outwards, ranging from 0·003 W m^{-2} to 0·075 W m^{-2}. The horizontal inhomogeneity of F is paralleled by a lateral inhomogeneity in the convective structures in the FOC. It appears that these inhomogeneities make the solution significantly more variable in space and time than the model 1 solution. This can be seen in figure 10, where a snapshot of the contours of B_r on the CMB are shown at a time of significant deviation. When compared with figure 8, it is particularly striking how much further the magnetic equator deviates from the geographic equator. This can also be seen in figure 11, where the axisymmetric parts of the field are shown (at the same instant as figure 10). The differences between figure 11 and figure 9 (which refers to model 1) are especially impressive. Experience with model 0 suggests that 'tongues' of flux, such as the one seen in figures 10 and 11, may be harbingers of a reversal, a possibility that we are pursuing at the present time. In answer to Q10, it is hard to resist the speculation that, when the Earth is in a regime of frequent reversal, as as the present stage of its evolution, it is because mantle convection has created large lateral variations in temperature on the CMB; when reversals are infrequent, as in the Permian or early Cretaceous, mantle convection may have produced a thermal structure in the lower mantle that does not involve large variations in heat flux over the CMB.

8.3. *Model 3*

This, the first subadiabatic model that we investigated, was something of a disappointment. It was studied over a period of 240 000 years. The magnetic field decreased systematically in a series of steps, on each of which the field intensity remained much the same. Each step was marked by a sharp decline in **B** until eventually **B** became too small to exert any significant Lorentz force on the fluid flow. The resulting hydrodynamic solution was then very similar to those derived in earlier hydrodynamic calculations, such as that of Glatzmaier and Olson (1993), in which convective activity is largely confined to the exterior, E of the tangent

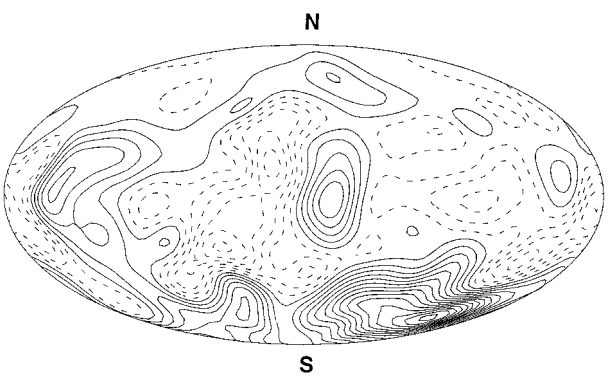

Figure 10. A snapshot of the radial component of the magnetic field produced by model 2 at the core–mantle boundary (equal area projection). The North (South) geographic pole is at the top (bottom) of the projection, the equator being a horizontal line through the middle. The field is directed outward (inward) on the solid (broken) contours. The maximum field intensity outward is 0·39 mT and inward is 0·18 mT.

cylinder. It seems clear that this model does not support a dynamo.

8.4. *Model 4*

The lateral inhomogeneities imposed in this, the second subadiabatic model, are so strong that the inward convective heat flux in some areas of the CMB exceeds the outward adiabatic flux, so that the net heat flux is actually inwards! The heat flux, $F(\theta,\phi,t)$, per unit area of the CMB ranges between 0·019 W m^{-2} inwards to 0·045 W m^{-2} outwards. The horizontal mean of the entropy S is shown in figure 12 for both the superadiabatic and subadiabatic models, and it is clearly seen that S increases outwards near the CMB for model 4, but that the deep FOC is on average superadiabatic (S increasing inwards). The structure of S determines the convective heat flux, which adds to the conductive heat flux. It is displayed in figure 13 through contours in the equatorial plane. It may be seen that the hot regions of inward heat flux are centred at longitudes 150° and 330°, which coincide with those seen in the snapshot of the CMB heat flux shown in figure 3, which was taken at the same time. (In that figure, longitude 0° is at the far left). The velocity and field patterns propagate westward so that they alternately move under areas of the CMB where the convective heat flux is outward, and areas where it is inward. This tends to suppress the outward flow in a way that is reminiscent of model 2; the snapshot of the contours of constant V_r in the equatorial plane shown in figure 14 was taken at the same instant of time as for figures 3 and 13.

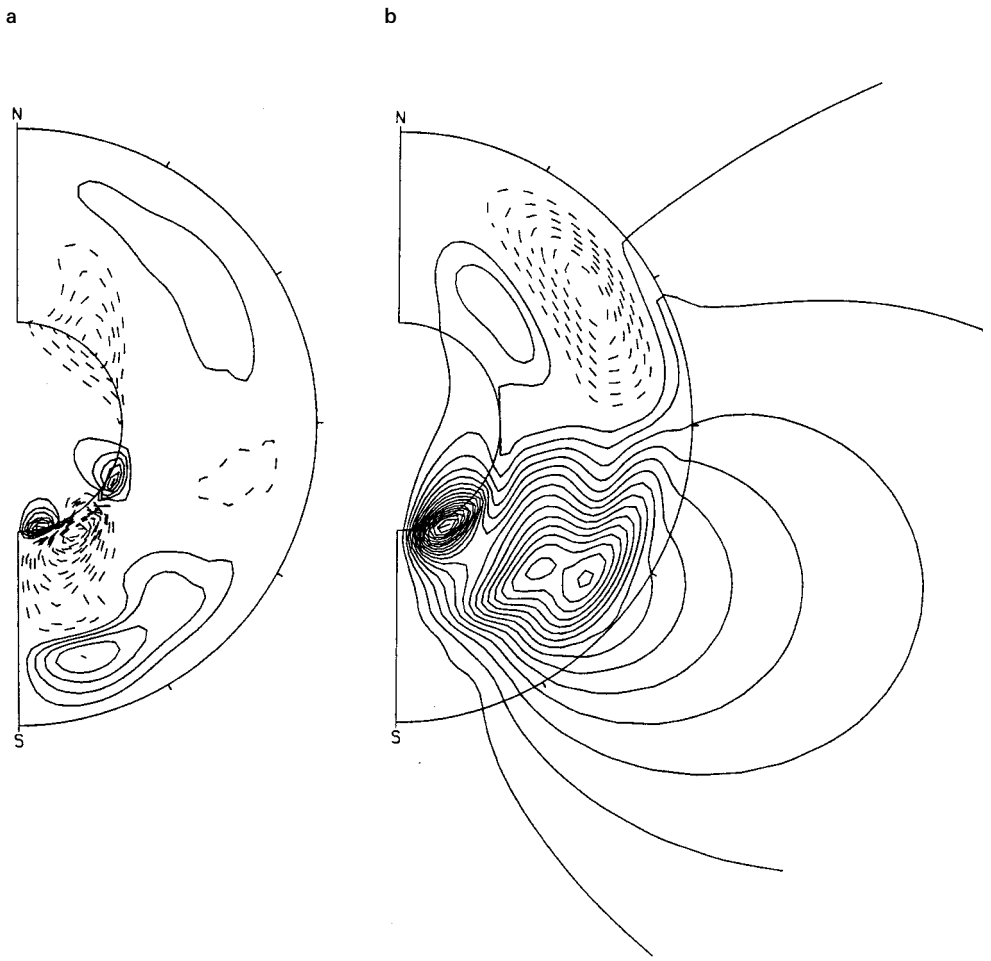

Figure 11. The longitudinal average of the three-dimensional magnetic field typically produced by model 2: (*a*) contours of the zonal field which has a maximum eastward component (shown by the solid curves) of 6 mT and a maximum westward component (shown by the broken curves) of 11 mT; (*b*) lines of force of the meridional field, which are directed counter-clockwise where shown as solid curves and clockwise where shown as broken curves; the maximum intensity is 18 mT.

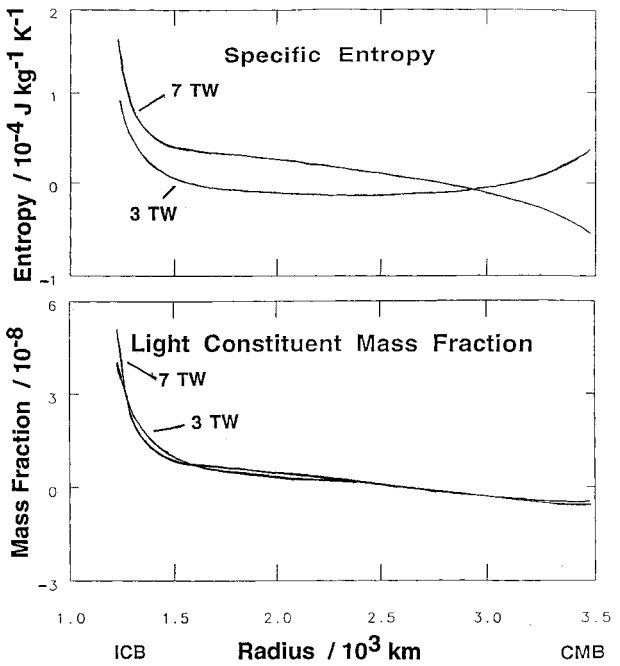

Figure 12. The horizontally-averaged specific entropy, $\bar{S}$, and light constituent fraction, ξ, as functions of radius, r, through the fluid outer core. In the 7·2 TW (3·0 TW) models, $\bar{S}$ has a negative (positive) radial gradient near and at the CMB. The homogeneous CMB heat flux models (1 and 3) are shown in this figure, but the heterogeneous models (2 and 4) have very similar profiles. The forms of $\xi(\bar{r})$ are similar in all the models.

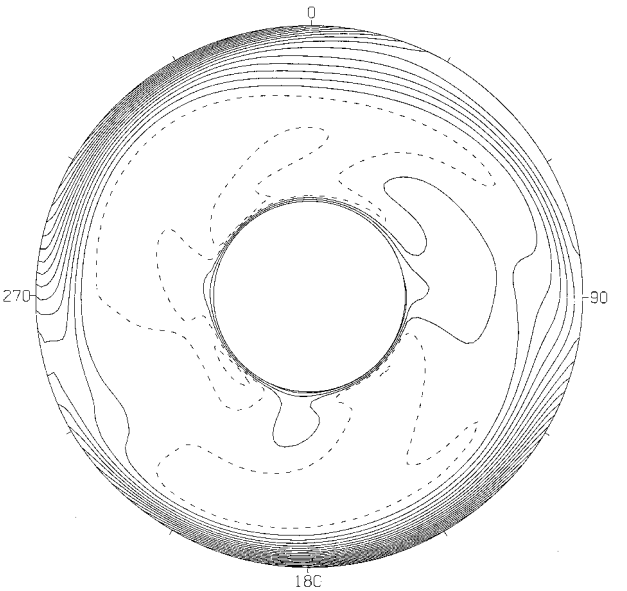

Figure 13. A snapshot of the contours of the specific entropy, S, for model 4. The curves shown are the intersections of the iso-entropy surfaces with the equatorial plane $\theta = \pi/2$, and refer to the same instant in time as figures 3 and 14. The equatorial plane is viewed from the South, so that the direction of the Earth's rotation is clockwise. Solid (broken) contours represent positive (negative) variations from a constant ($\bar{S}$). The difference between maximum and minimum values is $2{\cdot}1 \times 10^{-4}$ J kg^{-1} K^{-1}.

The field strength was roughly the same throughout the 200 000 years of the simulation, and it appears that, unlike model 3, this is another self-excited dynamo. The peak strength of **B** is consistently about 10 times less than for models 1 and 2 or for the Earth. In addition, the eastward rotation of the SIC is less than that of models 0–2; it is typically 0·5°/yr.

The reason why model 4 maintains a dynamo, when model 3 does not, presents an interesting puzzle. In some sense, there is nothing special about a spherical dynamo, and perhaps we may picture the regions of the core lying below the superadiabatic areas of the CMB (the areas where locally the net heat flux exceeds the adiabatic) as non-spherical field-generating volumes, interacting through the global zonal circulation and fields in the FOC and all contributing to the global geodynamo?

9. The future

It is only two years since Jacobs (1995) described 'The Earth's magnetic field' in the pages of this journal, and it will be apparent to anyone who compares his account with our own that the subject has changed enormously in the intervening period. At the time he wrote, no three-dimensional convective geodynamo simulations had been reported; by now several have been integrated and have generated magnetic fields that resemble the Earth's in encouraging ways. A polarity reversal has been simulated, and a new seismological target has been identified: to discover the evolution in time of the angular velocity of the inner core. This provides a new diagnostic tool with which to test the geophysical relevance of any geodynamo simulation. So far, our geodynamo models survive trial by this particular diagnostic. Although three of the five simulations (models 0, 1 and 2) generate magnetic fields resembling the Earth's in both structure and magnitude, some unanswered challenges remain. For example, why is the Boussinesq solution (model 0) so sensitive to the viscosity near the CMB? Such a behaviour makes one wonder whether viscous forces are as innocuous as we suggested in section 4. Evidently, numerical techniques are needed that will make simulations with much smaller viscosities possible.

The methods that have worked successfully in our simulations, should also be applicable to the early Earth (which had a smaller inner core), planets such as Venus (to obtain hints why this does not operate a dynamo) and Mercury (which does), and the Galilean satellites of Jupiter, at least one of which (Ganymede) appears to have a

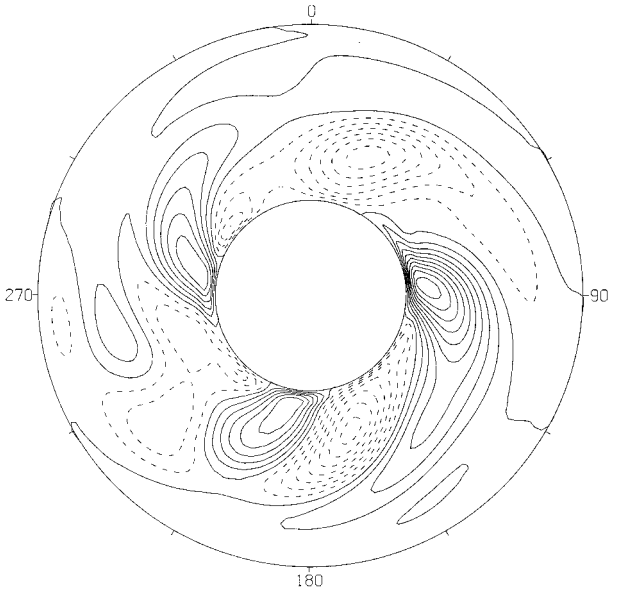

Figure 14. A snapshot of the contours of equal radial velocity, V_r, in model 4, plotted in the equatorial plane $\theta = \pi/2$, at the same time as the snapshots shown in figures 3 and 13. The equatorial plane is viewed from the South, so that the direction of the Earth's rotation is clockwise. Contours on which $V_r > 0$ are drawn with continuous lines; those on which $V_r < 0$ are drawn with broken lines. The maximum outward velocity is $4{\cdot}5 \times 10^{-4}$ m s^{-1}; the maximum inward velocity is $3{\cdot}5 \times 10^{-4}$ m s^{-1}.

dynamo operating within it. Whatever the future brings, it should be exciting!

Acknowledgements

The computing resources were provided by the Pittsburgh Supercomputing Center under grant MCA94P016P and the Advanced Computing Laboratory at the Los Alamos National Laboratory. Different aspects of this work were supported by Los Alamos LDRD Grant 96149, UCDRD Grant 9636, IGPP Grant 713, and by NASA Grant NCCS5-147. PHR was supported by NSF Grant EAR94-06002. The work was conducted under the auspices of the US Department of Energy, supported (in part) by the University of California, for the conduct of discretionary research by Los Alamos National Laboratory.

References

Alfvén, H., 1942, *Nature* **150,** 405.
Backus, G. E., 1958, *Ann. Phys.*, **4,** 372.
Bloxham, J., and Gubbins, D., 1985, *Nature*, **317,** 777.
Bloxham, J., and Jackson, A., 1992, *J. Geophs. Res.*, **97,** 19537.
Braginsky, S. I., 1963, *Sov. Phys. Dokl.*, **149,** 8.
Braginsky, S. I., 1964, *Geomagn. Aeron.*, **4,** 572.
Braginsky, S. I., 1993, *J. Geomag. Geoelec.*, **45,** 1517.
Braginsky, S. I., and Roberts, P. H., 1995, *Geophys. Astrophys. Fluid Dynam.*, **79,** 1.
Buffett, B. A., 1996, *Geophys. Res. Lett.*, **23,** 2279.
Chandrasekhar, S., 1961, *Hydrodynamic and Hydromagnetic Stability* (Oxford: Oxford University Press).
Cowling, T. G., 1933, *Mon. Not. R. astr. Soc.*, **94,** 39.
Dziewonski, A. M., and Anderson, D. L., 1981, *Phys. Earth Planet. Inter.*, **25,** 297.
Glatzmaier, G. A., 1984, *J. Comp. Phys.*, **55,** 461.
Glatzmaier, G. A., and Olson, P., 1993, *Geophys. Astrophys. Fluid Dynam.*, **70,** 113.
Glatzmaier, G. A., and Roberts, P. H., 1995a, *Phys. Earth Planet, Inter.*, **91,** 63.
Glatzmaier, G. A., and Roberts, P. H., 1995b, *Nature*, **377,** 203.
Glatzmaier, G. A., and Roberts, P. H., 1996a, *Physica D*, **97,** 81.
Glatzmaier, G. A., and Roberts, P. H., 1996b, *Science*, **274,** 1887.
Glatzmaier, G. A., and Roberts, P. H., 1996c, *Phys. Earth Planet. Inter.*, **98,** 207.
Glatzmaier, G. A., and Roberts, P. H., 1997, *Int. J. Eng. Sci.*, to appear.
Herzenberg, A., 1958, *Phil. Trans. R. Soc. Lond.*, **A250,** 543.
Hollerbach, R., 1994, *Proc. R. Soc. Lond.*, **A444,** 333.
Hollerbach, R., and Jones, C. A., 1993a, *Nature*, **365,** 541.
Hollerbach, R., and Jones, C. A., 1993b, *Phys. Earth Planet. Inter.*, **87,** 171.
Jacobs, J. A., 1953, *Nature*, **172,** 297.
Jacobs, J. A., 1995, *Contemp. Phys.*, **36,** 267.
Kuang, W., and Bloxham, J., 1996, *EOS*, **77,** No. 46, 697.
Langel, R. A., 1986, *Geomagnetism 1*, edited by J. A. Jacobs, (London: Academic Press).
Larmor, J., 1919, *Rep. Brit. Assoc. Adv. Sci.*, **1919,** 159.
Loper, D. E., 1978, *Geophys. J. R. Astr. Soc.*, **54,** 389.
Matthews, P. M., Buffett, B. A., Herring, T. A., and Shapiro, I. I., 1991, *J. Geophys. Res.*, **96,** 8219, 8243.
Roberts, P. H., 1989, *Encyclopedia of Solid Earth Geophysics*, edited by D. E. James, (New York: van Nostrand Reinhold) pp. 148 – 160.
Song, X., and Richards, P., 1996, *Nature*, **382,** 221.
Su, W., and Dziewonski, A. M., 1995, *J. Geophys. Res.*, **100,** 9831.
Su, W., Dziewonski, A. M., and Jeanloz, R., 1996, *Science*, **274,** 1883.
Tackley, P. J., Stevenson, D. J., Glatzmaier, G. A., and Schubert, G., 1994. *J. Geophys. Res.* **99,** 15877.

Gary Glatzmaier received his PhD from the University of Colorado. He is now a Fellow of the Los Alamos National Laboratory, and of the American Geophysical Union. He is presently a visiting Professor at UCLA. His research centres on three-dimensional numerical simulations of convection in the interiors of the sun and Jupiter and in the Earth's atmosphere, mantle and core.

Paul Roberts received his PhD and ScD, from Cambridge University, England, and was formerly a Professor at the University of Newcastle upon Tyne, England. He is now a Professor of Mathematics and of Geophysical Sciences at UCLA. He is a Fellow of the Royal Society, the Royal Astonomical Society and the American Geophysical Union.